

How Do Inhibitors Mitigate Corrosion in Oil-Water Two-Phase Flow Beyond Lowering the Corrosion Rate?

Chong Li,* Sonja Richter,†* and Srdjan Nešić*

ABSTRACT

Corrosion inhibitors are commonly used to mitigate corrosion in oil and gas pipelines, and the choice of inhibitor for a particular oil field depends on the conditions of the field (oil chemistry, water chemistry, temperature, etc.). To find the optimum formulation for each field condition, extensive laboratory tests are carried out, which include corrosion inhibitor performance, foaming, and emulsification, to name a few. However, corrosion inhibitors can have the additional advantage of altering the wettability of the steel surface from hydrophilic (water wet) to hydrophobic (oil wet) by forming a hydrophobic adsorption layer on the steel surface. In the current work, the ability of chemicals to alter the wettability of the steel is investigated by measuring the static contact angle in a goniometer, as well as the dynamic wetting with a small scale flow apparatus, called a doughnut cell, especially designed for this purpose. The doughnut cell makes it possible to measure the water and oil wetting of a steel surface using flush-mounted conductivity pins that detect whether water (conductive fluid) or oil (non-conductive fluid) are covering the surface. The two generic compounds tested here, a quaternary ammonium chloride and a fatty amine, lowered the corrosion rate, altered the surface wetting from hydrophilic (mostly water wet) to hydrophobic (mostly oil wet), and lowered the oil-water interfacial tension, facilitating water entrainment in the oil. A doughnut cell was used to map out how an inhibitor can increase the oil-wetting regime for a given water cut. It is a practical tool that can be used to help optimize the inhibitor dosage and maximize its value. It can also be used in new field development, where

enhanced oil wetting could be factored into the corrosion allowance calculation.

KEY WORDS: adsorption, carbon steel, CO₂ corrosion, corrosion inhibitors, wettability

INTRODUCTION

Adsorption and efficiency of corrosion inhibitors have been extensively researched for industrial application in the oil and gas industry, starting in the middle of the 20th century, most notably with the work of Hackerman beginning in 1948.¹ Publication in the literature on corrosion inhibitors has been steadily increasing and in the last 6 years has reached more than 500 publications a year. The research is nearly exclusively focused on the action of the corrosion inhibitor from the water phase only, ignoring the effect of the oil phase. However, the oil phase can enhance the performance of the chemical compound, as well as produce added protection by increased oil wetting and increased water entrainment.

A handful of researchers have looked at the effect of corrosion inhibitors on the steel surface wettability and/or interfacial tension. McMahon² observed how adding oleic imidazoline (OI) to the oil phase rendered the steel surface completely hydrophobic, resulting in droplets of water simply rolling off a steel disc. He also saw a drastic decrease in the oil-water interfacial tension with the addition of OI, reducing it to less than 1 mN/m with a concentration of only 10 ppm of OI.

Foss, et al., have investigated the effect of corrosion inhibitors on the wettability of corroded steel surface,³ iron carbonate (FeCO₃)-covered steel sur-

Submitted for publication: June 11, 2013. Revised and accepted: June 18, 2014. Preprint available online: June 25, 2014. doi: <http://dx.doi.org/10.5006/1057>.

† Corresponding author. E-mail: sonja.richter@conocophillips.com.

* Institute for Corrosion and Multiphase Technology, Ohio University, 342 West State Street, Athens, OH 45701

face,⁴ and ferric-covered steel surface.⁵ Both OI and phosphate ester were able to alter the wettability in water-in-oil contact angle measurements from hydrophilic to hydrophobic increasing the oil wetting, while cetyltrimethylammonium bromide (CTAB) made the surface increasingly water wet. However, for the oil-in-water contact angle measurement, only the oxidized ferric corrosion product layer became oil wet in the presence of an inhibitor.⁵ The authors also concluded that the corrosion inhibition of the surface could be greatly enhanced with an exposure to the oil phase as a result of the modification of the inhibitor film.

Schmitt and Stradmann⁶ conducted contact angle measurements by placing oil and water droplets on carbon steel specimens in a high-pressure test apparatus. The tests were performed under 75°C and 80°C and 5 bar carbon dioxide (CO₂). The testing fluids were different crude oils, a synthetic oil and brine with surfactants (inhibitors and demulsifiers) added into the system. The contact angle measurements were made on the clean surface and pre-corroded (6, 24, 48, and 72 h) surface. It was found that a clean carbon steel surface and a pre-corroded surface covered with FeCO₃ scale both show hydrophilic wetting properties. The addition of quaternary ammonium inhibitor under FeCO₃ scale formation conditions resulted in a hydrophilic surface; however, fatty amine and imidazoline-based inhibitors produced a hydrophobic surface.

The current paper seeks to separate and emphasize the multifaceted roles of corrosion inhibitors that act not only to reduce corrosion directly but also facilitate the entrainment of water and render the surface hydrophobic (oil wet).

EXPERIMENTAL PROCEDURES

Materials

Two generic inhibitor compounds were tested: a quaternary ammonium chloride (“quat”) and a fatty amine compound. The composition of the quaternary ammonium chloride solution, including methanol as solvent, is given in Table 1, and the composition of the generic fatty amine corrosion inhibitor solution is given in Table 2 with acetic acid and methanol used as solvents for the fatty amine compound. The model oil was LVT200[†] with the properties listed in Table 3. The model oil is a clear, light paraffinic distillate consisting of straight chain hydrocarbon (C9-C16) with C14 being the most common fraction. It does not contain any impurities that would affect the corrosion rate.⁷ Composition of the UNS G10180⁽¹⁾ steel is given in Table 4.

[†] Trade name.

⁽¹⁾ UNS numbers are listed in *Metals and Alloys in the Unified Numbering System*, published by the Society of Automotive Engineers (SAE International) and cosponsored by ASTM International.

TABLE 1

Composition of Quaternary Ammonium Chloride Inhibitor Package

Substance	Weight (%)
Quaternary ammonium chloride	60 to 80
Methanol	10 to 30

TABLE 2

Composition of Fatty Amine Inhibitor Package

Substance	Weight (%)
Fatty amine compound	60 to 80
Acetic acid	10 to 30
Methanol	5 to 10

TABLE 3

Properties of the Model Oil Used in the Research

Property	Parameter	Value
Density	ρ	825 kg/m ³
Viscosity @ 25°C	μ	2.0 mPa.s
Interfacial tension	σ	40 mN/m
Oil-in-water contact angle	θ	73°

TABLE 4

Elemental Composition of the Mild Steel (UNS G10180) Sample Used as a Rotating Cylinder Electrode

Elements	Weight (%)
C	0.19
Si	0.22
Cr	0.13
Ni	0.16
Mn	0.83
Cu	0.16

Corrosion Inhibition Measurements

The corrosion testing was performed in a 2 L glass cell using three electrodes: a rotating cylinder made out of UNS G10180 pipeline steel (Table 4) with an exposed surface area of 5.4 cm² as the working electrode, a silver/silver-chloride (Ag/AgCl) as the reference electrode located in a Luggin capillary tube, and a platinum ring as the counter electrode. The linear polarization resistance (LPR) technique was used to measure the corrosion rate.

The glass cell including the Ag/AgCl reference electrode and the platinum counter electrode was filled with 2.0 L of 1.0 wt% sodium chloride (NaCl) solution, deoxygenated by purging with CO₂ for 1.5 h to 2 h to reach an oxygen concentration below 25 ppb. The equilibrium pH of the test solution was 3.8 to 3.9 and was adjusted to pH 5.0 by adding a deoxygenated sodium bicarbonate (NaHCO₃) solution. The working electrode was polished with 400 grit and 600 grit silicon carbide (SiC) paper using isopropyl alcohol as the cooling fluid. After polishing, the working electrode was cleaned in an ultrasonic bath with isopropyl alco-

hol and air dried with a blower. It was then mounted on the rotating electrode holder and inserted into the glass cell maintaining a rotation speed of 1,000 rpm. The temperature of the test was maintained at 25°C.

A potentiostat was connected to the three electrodes, and the open-circuit potential was first monitored for 5 min to 10 min until it became stable. LPR technique was conducted at 30 min intervals throughout the test to measure the corrosion rate. The polarizing range was ± 5 mV from the open-circuit potential with a scanning rate of 0.125 mV/s. The measured polarization resistance, R_p , was compensated with the solution resistance, R_s , measured by the electrochemical impedance spectroscopy (EIS) technique. The B-value for calculating the corrosion rate from LPR measurement was evaluated with weight loss and potentiodynamic sweeps, and a value of 21 mV/decade was obtained for measurements without an inhibitor as well as with quaternary ammonium chloride. However, for the fatty amine measurements, the B-value was determined to be 31 mV/decade.⁸

The corrosion inhibitor was introduced into the cell with a syringe 1.5 h after the working electrode had been exposed to the solution, and separate experiments were made for inhibitor concentrations ranging from 0 to 200 ppm based on the total liquid volume (2 L). Two series of glass cell experiments were conducted:

- For the so-called “pure corrosion inhibition” tests, only the brine phase was present in the glass cell.
- For the “direct oil wet” tests, the paraffinic model oil was added on top of the brine (in 1:9 volumetric ratio), and the working electrode was periodically lifted up into the oil phase and left there for 5 min rotating at 1,000 rpm, and then returned to the water phase for electrochemical measurements.

Interfacial Tension Measurements

A DuNouy tensiometer was used to measure the changes of oil-water interfacial tension due to the addition of an inhibitor. The tensiometer had a platinum wire ring, which was immersed in the water phase. The oil phase was slowly added on top of the water phase. The platinum ring was pulled up and when it broke through the oil-water interface, the required force in units of dyne/cm (equal to the S.I. unit mN/m) could be read directly from the dial of the tensiometer.

Deionized water with 1 wt% NaCl was deoxygenated by purging CO₂ gas in a 500-mL breaker for 1 h and was adjusted to pH 5.0 by adding NaHCO₃. To control the water chemistry during the addition of an inhibitor, a plastic glove bag with CO₂ gas continuously purging was used. The corrosion inhibitor was added to a test tube that contained 15 mL oil and 15 mL brine (deionized water with 1 wt% NaCl) with

the concentration of inhibitor calculated based on the total volume of liquid. After the addition of an inhibitor, the test tube was shaken for a few minutes and then set still for a period of 1 day for the inhibitor to partition. At the end of the partitioning period, the oil and the water were transferred by syringes to a glass container for tensiometer measurements.

Contact Angle Measurements

The contact angle measurements were conducted with the custom built goniometer, which can measure both the contact angle of an oil droplet sitting on a steel surface in a continuous brine phase (oil-in-water contact angle) and the contact angle of a water droplet suspended on a steel surface in a continuous oil phase (water-in-oil contact angle). Since both of the inhibitors described in this study were predominantly water soluble, the results presented below focus on the oil-in-water contact angle. The contact angle is always measured through the water phase and a larger contact angle ($>90^\circ$) indicates a hydrophobic (preferentially oil wet) surface, while a low contact angle ($<90^\circ$) indicates a hydrophilic (preferentially water wet) surface.

A carbon steel coupon was polished and placed on a polytetrafluoroethylene (PTFE) sample holder inside the goniometer vessel. The videos of the droplet were analyzed by an image-analyzing software and the contact angle, θ , was calculated according to Equation (1), where R is the radius of the droplet and L is the length of the contact line, both of which are provided by the image-analyzing software in the unit of pixels:

$$\theta = 180 - \arcsin\left(\frac{L}{2R}\right) \cdot \frac{180}{\pi} \quad (1)$$

For the contact angle tests, the vessel of the goniometer was filled with 500 mL of deionized water with 1 wt% NaCl. A sparger was inserted into the liquid to purge CO₂ gas for deoxygenation. The pH of the brine phase was adjusted to 5.0 with NaHCO₃. A flat API 5L X65 carbon steel sample was polished with 400- and 600-grit SiC paper, washed with isopropanol, and dried with a hot air blower. After the sample was immersed into the water phase, an oil droplet was placed underneath the surface using a 10- μ L syringe. A baseline test (without inhibitor) was carried out first and then the corrosion inhibitor was injected into the continuous water phase measurements taken and the concentration was increased stepwise.

Procedure for Dynamic Wetting Measurements

A benchtop apparatus, called a doughnut cell, was developed to simulate oil-water pipe flow on a small scale. The main purpose of the doughnut cell was to determine the occurrence of oil vs. water wetting at the bottom of a pipe, at a given water cut and

oil velocity, and it can also be used for corrosion rate measurements. A schematic of the cross section of the doughnut cell is given in Figure 1. Oil and water are introduced into the annulus at a given ratio and the flow is introduced by rotating the top lid, which shears the oil phase, which, in turn, shears and possibly entrains the water phase. Series of conductivity pins⁹ are flush-mounted at the stainless steel (Type 316 [UNS S31600]) bottom of the channel, to detect whether water or oil is wetting the bottom.

The doughnut cell is conceptually similar to a “carousel” apparatus.¹⁰ Some of the disadvantages of the design, including secondary flow due to the rectangular cross section, have been minimized by using a computational fluid dynamics (CFD) model.⁸ The width of the annulus is 46 mm and it sits between a 0.46 m outer diameter (OD) (wall thickness 6 mm) and a 0.35 m OD (wall thickness 2.5 mm) acrylic cylinders. The height of the annulus is adjustable and was set at 70 mm, which resulted in a working volume of 4.2 L. Since the cross section of the channel is rectangular, the hydraulic diameter was calculated according to Equation (2), with H being the height (mm) and W the width (mm) of the annulus.

$$D_H = \frac{2 \cdot H \cdot W}{H + W} \quad (2)$$

A pitot tube was used to measure the oil phase velocity during testing. It was inserted into the cell through the bottom and used for measuring in situ circumferential velocity of the oil phase. The pitot tube was connected to a differential pressure transducer. The measured differential pressure, Δp (psi), can be converted to fluid velocity, u (m/s), according to Bernoulli's equation [Equation (3)], in which 6,894.76 is a unit conversion factor for pressure from psi to Pa and ρ_{fluid} is the density of the fluid (kg/m^3), which, in this case, is the density of the model oil ($825 \text{ kg}/\text{m}^3$).

$$u = \sqrt{\frac{2 \cdot \Delta p \cdot 6,894.76}{\rho_{\text{fluid}}}} \quad (3)$$

The volume of water and oil, which are placed into the channel, are determined based on the desired water cut. Water was first poured into the cell from the top and then the oil was added. The measurement point for the pitot tube was in the middle of the oil phase, though when the water is entrained, it is possible that it can influence the velocity measurements. The test started at low rotational speeds, which gave low oil velocity, and a conductivity pin measurement was carried out. The rotation was then stopped and the oil and water were allowed to separate before the rotation speed was set to give a higher velocity. This was repeated until all the water from the bottom was entrained and oil wetting had been detected by the conductivity pins. The whole procedure was repeated

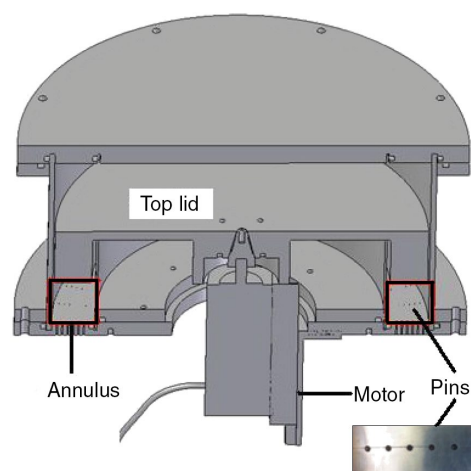


FIGURE 1. Cross section of the doughnut cell benchtop apparatus with the annulus indicated in black squares and a close-up of the conductivity pins at the bottom that detect water or oil at the surface. The annulus is filled with liquid, which is rotated with the top lid.

for different water cuts until a full-phase wetting map was created.

All the different pieces of equipment used in the present research (glass cell, tensiometer, goniometer and doughnut cell) were thoroughly cleaned after each test with tap water, deionized (DI) water, and isopropyl alcohol in succession, to avoid inhibitor cross-contamination.

RESULTS

Corrosion Inhibition

Figure 2(a) shows the pure corrosion inhibition (from water phase only) obtained by adding increasing concentrations of quaternary ammonium chloride to the water phase. The corrosion rate steadily decreased as the concentration of inhibitor was increased and a fairly high concentration was needed to produce a significant corrosion inhibition within the first few hours of testing. It took about 10 h for the corrosion rate to go down to 0.1 mm/y for the quaternary ammonium chloride at 200 ppm. On the other hand, the fatty amine inhibitor (Figure 2(b)) reduced the corrosion rate to 0.1 mm/y in 1 h for 200 ppm concentration and a concentration of 20 ppm and higher were sufficient to reach such a low corrosion rate (0.1 mm/y).

Figure 3 shows the result of exposing the corrosion sample periodically to a model oil (direct oil wet). In the case of quaternary ammonium chloride (Figure 3(a)), there was no effect of exposing the sample to the oil phase, neither at 5 ppm concentration as shown in Figure 3(a), nor at any other higher concentration.⁸ However, in the case of the fatty amine inhibitor (Figure 3(b)), there was a dramatic drop in the corrosion rate as the sample was exposed to the oil phase, even though the model oil is composed of straight chain hydrocarbon molecules, which do not have an affi-

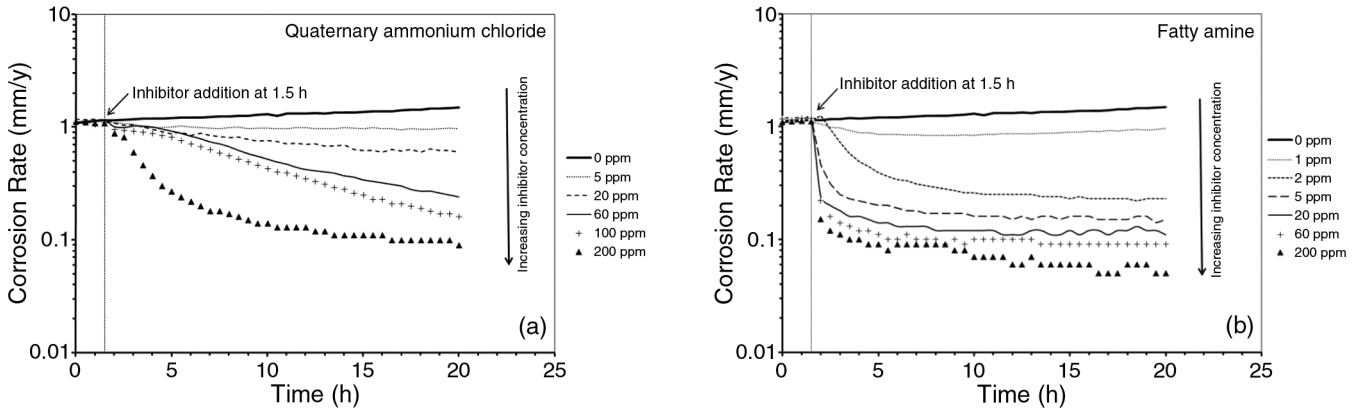


FIGURE 2. Inhibition of corrosion after the addition of (a) quaternary ammonium chloride and (b) fatty amine at various concentrations. The vertical dotted line at 1.5 h indicates the addition of the inhibitor to the water phase.

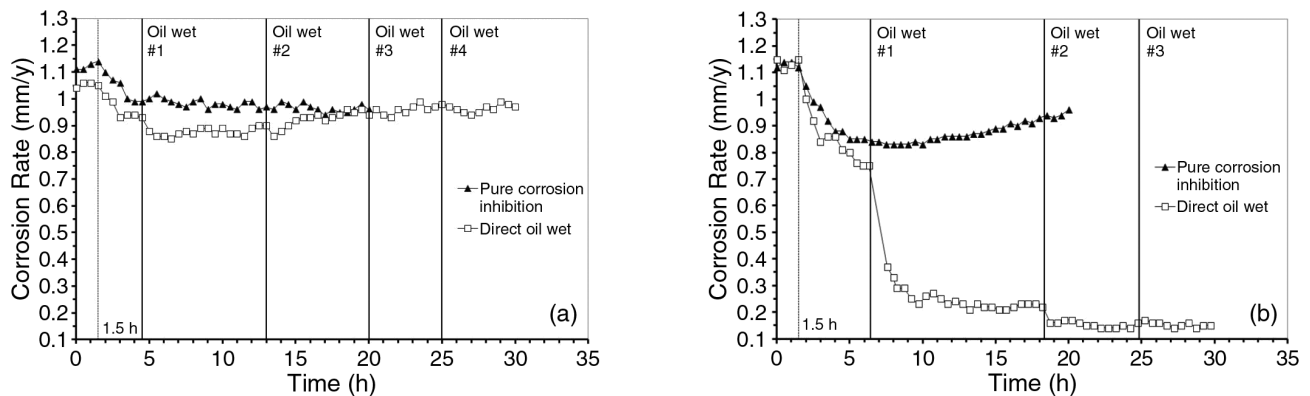


FIGURE 3. Direct oil-wet test for (a) quaternary ammonium chloride at 5 ppm concentration and (b) fatty amine inhibitor at 1 ppm concentration. The dotted line at 1.5 h notes when the inhibitor was added to the water phase and the solid lines note when the sample was exposed to the oil phase.

ity to adsorb on the steel surface, and do not directly affect the corrosion process.⁷ After only a short exposure (5 min) to the inert model oil, the corrosion rate dropped from 0.75 mm/y to 0.37 mm/y and settled at 0.2 mm/y. A subsequent exposure to the oil phase resulted in a slight decrease in the corrosion rate to 0.15 mm/y, but further exposure to the oil phase did not affect the corrosion rate.

Interfacial Tension

Corrosion inhibitors do not only gather at the steel-water interface, they can also gather at the oil-water interface and subsequently lower the interfacial tension. The interfacial tension between the model oil and the water phase was measured to be 40 mN/m. Figure 4(a) shows that even at low inhibitor concentrations the interfacial tension can be significantly reduced. Only 1 ppm of fatty amine was enough to lower the interfacial tension to 21.9 mN/m. The interfacial tension dropped fairly rapidly for the lowest concentrations of inhibitor but then started to level off as the concentration was increased further. The concentration at which the interfacial tension started to level off

is called the critical micelle concentration (CMC) and denotes the concentration at which the oil-water interface becomes saturated with inhibitor and micelles start to form in the liquid phase. The CMC was very similar for the two chemical compounds: for fatty amine it was measured to be 3 ppm and for quaternary ammonium chloride 5 ppm. The interfacial tension at the CMC is about 5 mN/m for both of the inhibitors.

Since the water phase is heavier than the oil phase, the water phase tends to settle at the bottom of the pipe, but sufficient turbulent energy of the flow can overcome the gravitational effect and entrain the water. In the process of entraining the water, it is broken up into droplets and the efficiency of this process depends on the interfacial tension. Therefore, lower interfacial tension makes water droplet breakup easier and facilitates the entrainment of water. To illustrate this effect, which is hard to measure directly, a water-wetting model¹¹ was used to predict the transition between oil and water wetting, depending on the oil properties, geometric factors, and flow rates of oil and water. The pipe diameter used for the simulation here was the hydraulic diameter of the rectangular

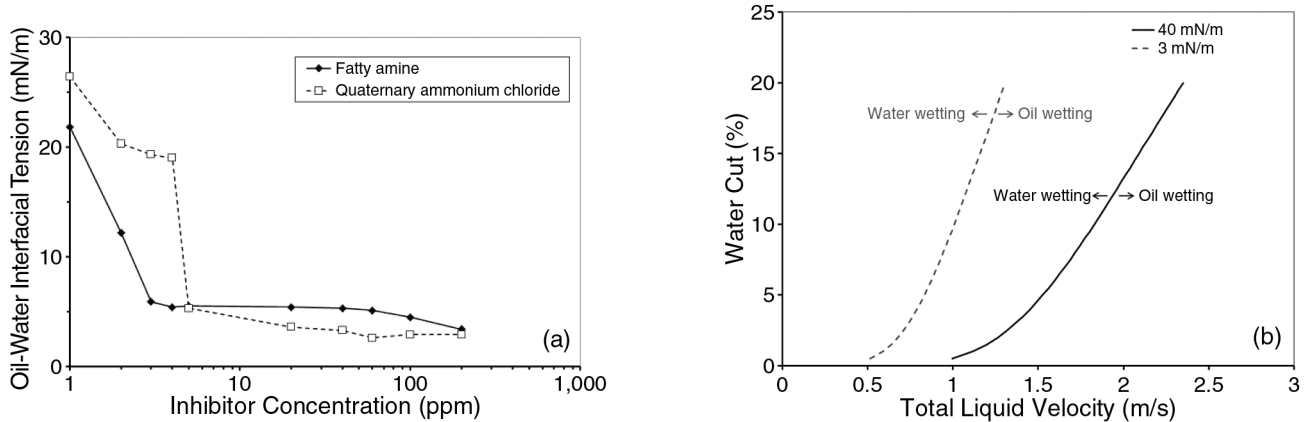


FIGURE 4. (a) Interfacial tension of model oil and water with the addition of increasing concentration of inhibitor. (b) Predicted transition between oil wetting and water wetting at high (40 mN/m) interfacial tension and low (3 mN/m) interfacial tension. Other oil properties were kept constant ($\rho = 825 \text{ kg/m}^3$, $\mu = 2.0 \text{ mPa}\cdot\text{s}$, $\theta = 73^\circ$, $D = 0.0555 \text{ m}$, $\beta = 0^\circ$). On the right of the transition, oil wetting is predicted; on the left, water wetting is predicted.

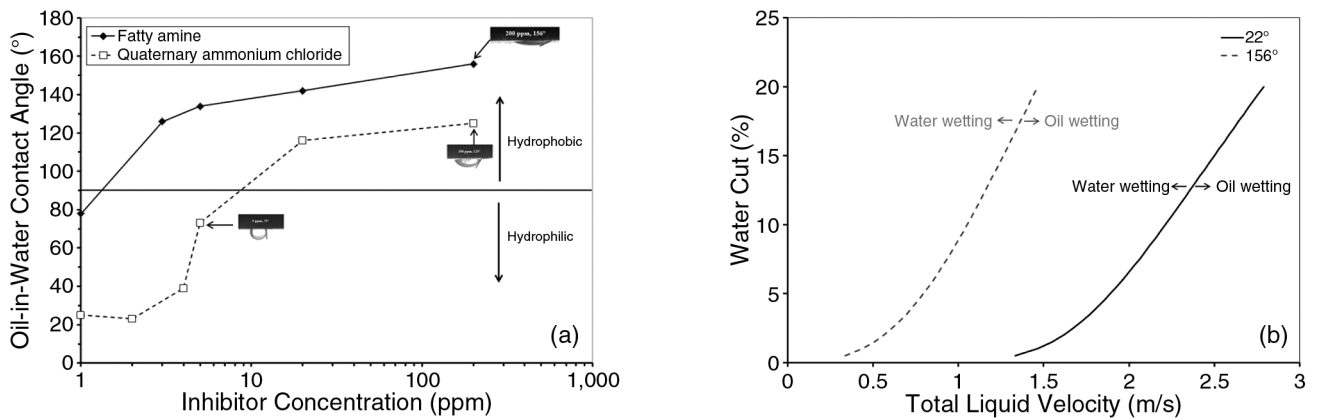


FIGURE 5. (a) Oil-in-water contact angle for fatty amine and quaternary ammonium chloride. The images show the corresponding oil droplet. (b) Predicted transition between oil wetting and water wetting at low (22°) contact angle and high (156°) contact angle. Other oil properties were kept constant ($\rho = 825 \text{ kg/m}^3$, $\mu = 2.0 \text{ mPa}\cdot\text{s}$, $\sigma = 40 \text{ mN/m}$, $D = 0.0555 \text{ m}$, $\beta = 0^\circ$). On the right of the transition, oil wetting is predicted and on the left, water wetting is predicted.

cross-sectional doughnut cell channel (calculated to be 0.0555 m). The resulting transition from water to oil wetting is shown in Figure 4(b) for water cuts less than 20%. The total liquid velocity refers to the combined superficial velocity of oil and water.

By altering only the interfacial tension in the model and keeping the other required parameters constant, it is possible to see the effect of the interfacial tension independent of other parameters. As can be seen in Figure 4(b), by lowering the interfacial tension from 40 mN/m to 3 mN/m, the transition to oil wetting occurred at a much lower velocity. For instance, at 10% water cut, the transition occurred at 1.8 m/s when the interfacial tension is 40 mN/m, but at 1.1 m/s when the interfacial tension is 3 mN/m. The beneficial effects of corrosion inhibitors is not only to promote corrosion inhibition by adsorption but also to keep the water entrained in the oil rather than corroding the pipe surface.

Contact Angle

The contact angle is a measurement of the static surface wettability. The oil-in-water contact angles for different concentrations of fatty amine and quaternary ammonium chloride are shown in Figure 5(a). The contact angle for a pure model oil was 22° (which denotes hydrophilic behavior) and with the addition of increasing concentration of fatty amine inhibitor, the contact angle increased rapidly, giving a hydrophobic contact angle ($>90^\circ$) with only 3 ppm concentration, which is the CMC for fatty amine.⁸ The contact angle did not increase as rapidly for quaternary ammonium chloride, and did not become hydrophobic until the concentration about doubled the CMC (which is 5 ppm for the quaternary ammonium chloride). Furthermore, the contact angle for the quaternary ammonium chloride was always lower than that of the fatty amine, reaching 125° at 200 ppm concentration, compared to 156° for fatty amine at the same concentration. This

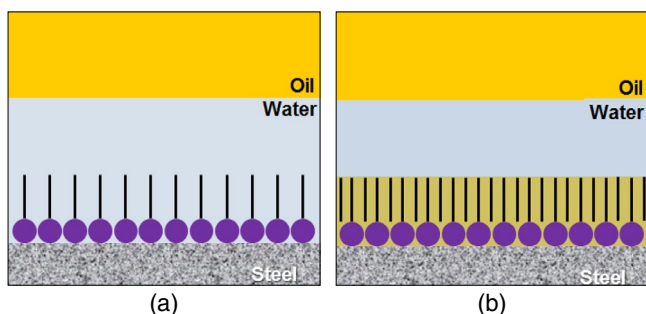


FIGURE 6. Illustration of the adsorption scenario of a regular monolayer of an oil soluble inhibitor (a) before and (b) after exposure to the oil phase. Inhibitor molecules are drawn as filled circles (head group) with a black line for the tail. The alkane molecules are depicted as black lines in between the tails of the inhibitor molecules.

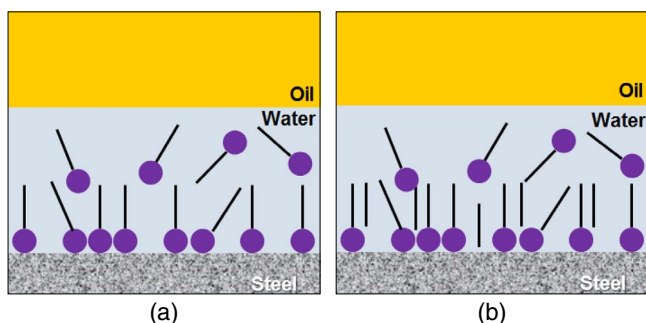


FIGURE 7. Illustration of the adsorption scenario of an irregular monolayer of a water soluble inhibitor (a) before and (b) after exposure to the oil phase. Inhibitor molecules are drawn as filled circles (head group) with a black line for the tail. The alkane molecules are depicted as black lines.

suggests that although the quaternary ammonium chloride does adsorb at the steel surface, it is not as efficient as fatty amine to form a hydrophobic layer.

The images incorporated into Figure 5(a) show how the higher contact angles corresponded to the increased spreading of the oil droplet on the steel surface. The increasing hydrophobicity of the steel surface with the addition of inhibitor is in contrast with the results of Foss, et al.³⁻⁵ With the exception of the oxidized (energized) surface,⁵ the water-in-oil contact angle measurement always gave a hydrophilic surface. The most plausible explanation for the difference between the Foss study and the current research is that in the current study the contact angle was measured with a freshly polished sample, while in the Foss study the sample was pre-corroded for 24 h before the contact angle measurement was conducted. The precorrosion can expose the cementite phase of the carbon steel, which can trap water, which promoted the hydrophilicity on the steel surface.

It can be concluded that besides providing direct corrosion inhibition and increasing the likelihood of water entrainment, corrosion inhibitors can also pro-

vide corrosion protection by making the steel surface more hydrophobic and thereby facilitating oil wetting of the steel surface. The predicted transition from water wetting to oil wetting, illustrating the effect of fatty amine, using the previously developed water wetting model,¹¹ can be seen in Figure 5(b). It shows the transition as a function of the oil-in-water contact angle for a pure model oil-water system (contact angle 22°) as well as the transition corresponding to the contact angle after an addition of 200 ppm of fatty amine into the water phase (156°). Higher contact angles make it easier to achieve oil wetting due to increased spreading of the oil on the surface. In this case at 10% water cut, the critical transition velocity is 2.3 m/s without the inhibitor, and 1.4 m/s with 200 ppm of the corrosion inhibitor.

DISCUSSION

The corrosion inhibition and contact angle study of the two chemicals presented in this paper showed two different behaviors, pointing to different adsorption mechanisms. The quicker and more efficient inhibition by the fatty amine compound, along with its immediate hydrophobic effect, suggests that the fatty amine inhibitor readily forms a hydrophobic layer at the steel surface, with the hydrophilic head group of the compound adsorbed on the surface and the hydrophobic tail pointed to the bulk solution (Figure 6). When the steel surface is exposed to the inert model oil, the alkane molecules (C12-C17) that make up the oil phase can line up with the hydrocarbon tails of the fatty amine molecules on the surface (Figure 6[b]) and thus strengthen the “monolayer” even further (hence the drop in corrosion rate).

On the other hand, the adsorption by the quaternary ammonium chloride seemed to be much slower according to the corrosion inhibition measurements, and a hydrophobic layer was not easily formed according to the contact angle measurements. Furthermore, the quaternary structure of the inhibitor molecule suggests that there could be steric effects hindering efficient formation of a hydrophobic layer. Figure 7 shows a hypothetical example of an irregular adsorbed layer. Exposing the layer to the oil phase does not significantly improve the inhibitor performance (Figure 3[a]) because the alkane molecules from the oil are not properly anchored between the tails of the inhibitor molecules (Figure 7) since they are not as regular. This can explain why exposing the steel surface to the model oil does not increase the corrosion inhibition in this case.

Doughnut Cell

The doughnut cell enables measurements of the dynamic wetting of the steel surface, which takes both the fluid flow (velocity, wall shear stress) into account, as well as the effect of water entrainment (interfacial

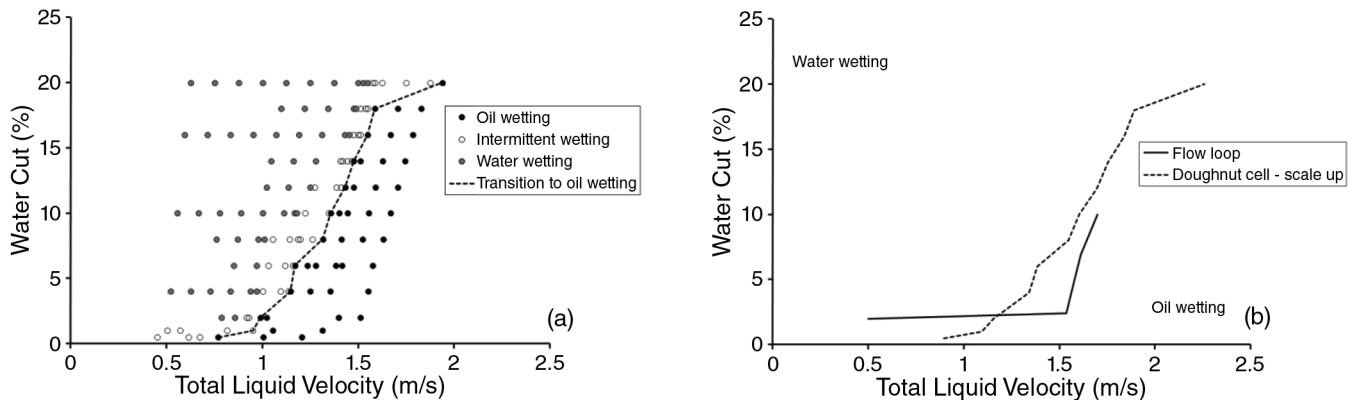


FIGURE 8. (a) Phase wetting map for model oil ($\rho = 825 \text{ kg/m}^3$, $\mu = 2.0 \text{ mPa}\cdot\text{s}$, $\sigma = 40 \text{ mN/m}$) made using the doughnut cell. The broken line shows the transition between oil wetting and non-oil wetting. (b) Comparison of the transition lines for model oil tested in the flow loop (full line) and the doughnut cell (broken line). To compare the transition lines directly for flow in two different geometries, the doughnut cell transition line has been scaled up using the water wetting model.⁹

tension) and oil spreading on the surface (contact angle). The doughnut cell can provide data for constructing a phase-wetting map, which displays the pattern of wetting as a function of water cut (%) and the flow velocity, as seen in Figure 8(a) for the model oil used here. There are three main wetting patterns detected, which are shown in Figure 8(a):

- oil wetting**, where all of the conductivity pins show oil wetted
- water wetting**, where at least some of the conductivity pins are permanently water wetted
- intermittent wetting**, where some of the conductivity pins are changing from oil to water wetting and vice-versa

The wetting map in Figure 8(a) showed that there is a threshold liquid velocity that needs to be reached before oil wet conditions were achieved and all the water is entrained. This threshold increased as the water cut is increased, going from, for example, 0.8 m/s for a 0.5% water cut to 1.9 m/s for a 20% water cut. The empirical transition line between oil wetting and intermittent wetting shown Figure 8(a) is considered to be the transition line from non-corrosive to corrosive conditions. A previous study⁹ showed that corrosion was not detected during oil-wetting conditions and that the corrosion rate during intermittent-wetting conditions was roughly half of the corrosion rate seen under full water-wetting conditions.

There are a number of differences in the fluid mechanics in the doughnut cell when compared to pipe flow:

- There is a difference in the shape of the cross section between the doughnut cell's rectangular channel and the circular cross section of a pipe.
- Pipe flow is typically straight and the doughnut cell flow is circular.
- Doughnut cell flow is a shear driven couette type flow, while pipe flow is pressure driven, etc.

Despite the difference between the two measurement devices, the transition line was remarkably similar as can be seen in Figure 8(b). Since the hydraulic diameter of the doughnut cell is roughly half the diameter of the flow loop, it was necessary to scale up the results of the doughnut cell to be able to compare it directly to the flow loop results. The scale up was performed by using the previously developed water-wetting model,¹¹ to isolate the effect of the diameter, where the predicted change in the transition velocity from one diameter to another was assumed to be the same as the empirical change in the transition velocity. This relatively crude method to scale up the results from the doughnut cell to the flow loop gave good results as seen in Figure 8(b), which shows the transition line for the flow loop data compared with the scaled up transition line of the doughnut cell. Later CFD work, which is still in progress, indicates that the reason why this scale up method seems to be applicable is that the velocity profile, at least from the bottom to the center point of the annulus, is remarkably similar to that of the flow loop. However, for a general application and as a proof-of-concept, a more in-depth fluid mechanics study is needed to take into account other flow parameters, such as the shear stress and the boundary layer thickness, etc., to have a comprehensive scale up method.

The doughnut cell was used to study how the surface wetting would change with the addition of an inhibitor. Figure 9 shows the empirical transition lines to oil wetting with the addition of quaternary ammonium chloride inhibitor. The oil-wetted area became increasingly larger (i.e., extended to lower liquid velocities) as the concentration of the inhibitor was increased. There was a large shift of the transition for concentrations up to the CMC (5 ppm). Increasing the inhibitor concentration above the CMC (up to 20 ppm) did not significantly alter the surface wetting since the surface was already saturated with the adsorbed in-

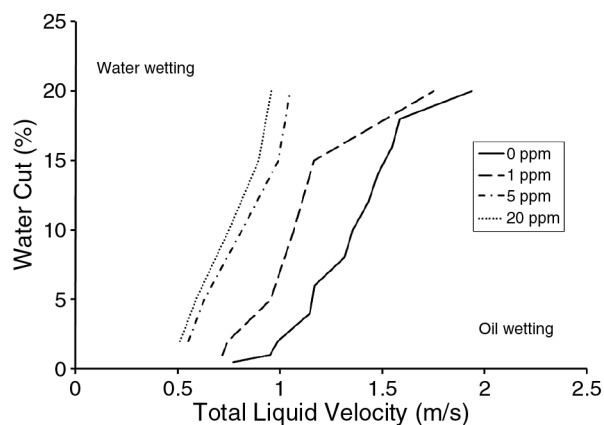


FIGURE 9. Transition from water to oil wetting with the addition of 1 ppm, 5 ppm, and 20 ppm quaternary ammonium chloride in the doughnut cell.

hibitor. Even if the adsorption mechanism of this inhibitor is slow and inefficient at low concentrations, it can still mitigate the corrosion by enhancing water entrainment (lower interfacial tension) and facilitating oil spreading at the steel surface (higher contact angles).

CONCLUSIONS

- ❖ The measurements of the contact angle for the two generic inhibitors tested suggest that the quaternary ammonium chloride does not form as strong an adsorption layer on the steel surface as the fatty amine does and is therefore not as effective in hindering access of water and dissolved corrosive species to the steel surface.
- ❖ Beyond lowering the corrosion rate, both inhibitors can lower the oil-water interfacial tension, making it easier for the water to be entrained in the oil flow.
- ❖ Both inhibitors can increase the oil wettability of the steel surface, making it harder for water to come into direct contact with the steel. This will decrease the likelihood of corrosion.
- ❖ The doughnut cell is a newly developed benchtop scale apparatus that can be used to simulate oil-

water flow on a relatively small scale, saving both time and cost associated with large-scale flow loop studies.

- ❖ The doughnut cell can provide measurements of the transition to oil wetting and it can be used to help optimize the inhibitor dosage in oil-water flow conditions.
- ❖ It was found that oil wetting did not increase significantly beyond the CMC concentration.

ACKNOWLEDGMENTS

The authors would like to thank A. Schubert, the Laboratory Director at the Institute for Corrosion and Multiphase Technology (ICMT), for assistance in the design of the doughnut cell. The financial support of the consortium of companies participating in the Water Wetting Joint Industry Project at ICMT, Ohio University, is greatly appreciated. The companies are BP, ConocoPhillips, ENI, ExxonMobile, Petrobras, Saudi Aramco, Shell, and Total.

REFERENCES

1. N. Hackerman, *Corrosion* 4, 2 (1948): p. 45-60.
2. A.J. McMahon, *Colloids Surf.* 59(C) (1991): p. 187-208.
3. M. Foss, E. Gulbrandsen, J. Sjöblom, *Corrosion* 64, 12 (2008): p. 905-919.
4. M. Foss, E. Gulbrandsen, J. Sjöblom, *Corrosion* 65, 1 (2009): p. 3-14.
5. M. Foss, E. Gulbrandsen, J. Sjöblom, *Corrosion* 66, 2 (2010): p. 025005-025005-11.
6. G.A. Schmitt, N. Stradmann, "Wettability of Steel Surfaces at CO₂ Corrosion Conditions. I. Effect of Surface Active Compounds in Aqueous and Hydrocarbon Media," CORROSION/98, paper no. 28 (Houston, TX: NACE International, 1998).
7. S. Yang, W. Robbins, S. Richter, S. Nešić, "Evaluation of the Protectiveness of Paraffins for CO₂ Corrosion," CORROSION/12, paper no. C2012-0001323 (Houston, TX: NACE, 2012).
8. C. Li, "Effect of Corrosion Inhibitor on Water Wetting and Carbon Dioxide Corrosion In Oil-Water Two Phase Flow" (Diss., Ohio University, Athens, OH, 2009).
9. J. Cai, C. Li, X. Tang, F. Ayello, S. Richter, S. Nešić, *Chem. Eng. Sci.* 73, 0 (2012): p. 334-344.
10. B.F.M. Pots, J.F. Hollenberg, E.L.J.A. Hendriksen, "What are the Real Influences of Flow on Corrosion?," CORROSION/2006, paper no. 06591 (Houston, TX: NACE, 2006).
11. X. Tang, S. Richter, S. Nešić, "A New Improved Model for Phase Wetting Prediction in Oil-Water Two Phase Flow," CORROSION/2013, paper no. C2013-0002393 (Houston, TX: NACE, 2013).